# Intrinsic neural timescales mediate the cognitive bias of self – temporal integration as key mechanism

Angelika Wolman [a,b,*], Yasir Çatal [b], Annemarie Wolff [b], Soren Wainio-Theberge [c,d], Andrea Scalabrini [e], Abdessadek El Ahmadi [f], Georg Northoff [b,g,h,i]

[a] School of Psychology, University of Ottawa, 136 Jean-Jacques Lussier, Ottawa, ON K1N 6N5, Canada
[b] Mind, Brain Imaging and Neuroethics Unit, Institute of Mental Health Research, Royal Ottawa Mental Health Centre, University of Ottawa, 1145 Carling Avenue, Ottawa, ON K1Z 7K4, Canada
[c] Integrated Program in Neuroscience, McGill University, Montreal, QC, Canada
[d] Douglas Mental Health University Institute, 6875 Boulevard LaSalle Rm. F-1146, Montréal, QC H4H 1R3, Canada
[e] Department of Human and Social Sciences, University of Bergamo, Bergamo, Italy
[f] Laboratoire de Neurosciences Cognitives, LNC UMR 7291, Aix Marseille Université-CNRS, Marseille 13331, France
[g] Centre for Neural Dynamics, Faculty of Medicine, University of Ottawa, Roger Guindon Hall, 451 Smyth Road, Ottawa, ON K1H 8M5, Canada
[h] Mental Health Centre, Zhejiang University School of Medicine, 866 Yuhangtang Rd, Hangzhou 310058, China
[i] Centre for Cognition and Brain Disorders, Hangzhou Normal University, Tianmu Road 305, Hangzhou 310013, China

## ARTICLE INFO

## ABSTRACT

Our perceptions and decisions are not always objectively correct as they are featured by a bias related to our self. What are the behavioral, neural, and computational mechanisms of such cognitive bias? Addressing this yet unresolved question, we here investigate whether the cognitive bias is related to temporal integration and segregation as mediated by the brain's Intrinsic neural timescales (INT). Using Signal Detection Theory (SDT), we operationalize the cognitive bias by the Criterion C as distinguished from the sensitivity index d'. This was probed in a self-task based on morphed self- and other faces. Behavioral data demonstrate clear cognitive bias, i.e., Criterion C. That was related to the EEG-based INT as measured by the autocorrelation window (ACW) in especially the transmodal regions dorsolateral prefrontal cortex (dlPFC) and default-mode network (DMN) as distinct from unimodal visual cortex. Finally, simulation of the same paradigm in a large-scale network model shows high degrees of temporal integration of temporally distinct inputs in CMS/DMN and dlPFC while temporal segregation predominates in visual cortex. Together, we demonstrate a key role of INT-based temporal integration in CMS/DMN and dlPFC including its relation to the brain's uni-transmodal topographical organization in mediating the cognitive bias of our self.

## 1. Introduction

The self is a core feature of our mental life and plays an important role in perception, action, and cognition. The mediation of our personal preferences and the cognitive strategies adopted under uncertainty are key sources by which the self exerts a bias on our cognitive processes (Amodeo et al., 2021; Barton et al., 2021; Nijhof et al., 2020; Sparks et al., 2016; Sui and Humphreys, 2015). Humans are subjected to such cognitive bias in the sense that self-specific stimuli are differently treated compared to non-self-specific information (Sui and Humphreys, 2015; Christoff et al., 2011; Northoff, 2011; Northoff et al., 2006). In particular, self-specific stimuli induce a benefit in response time and precision in diverse tasks (Jiang et al., 2019; Sui et al., 2012) and are more easily remembered (for an overview, see

(Cunningham and Turk 2017)). On the neural side, several studies have linked self-referential processing to the higher-order regions like cortical midline structures (CMS, (Frewen et al., 2020; Kelley et al., 2002; Murray et al., 2012; Northoff and Bermpohl, 2004; Qin et al., 2020)), the dorsolateral prefrontal cortex (dlPFC), and the default mode network (DMN, (Frewen et al., 2020; Kolvoort et al., 2020; Qin and Northoff, 2011). What are the behavioral, neural and computational mechanisms by which the CMS/DMN mediate the cognitive bias? Addressing this yet unresolved question is the goal of our study.

Decision making is a complex process. When we have to make a decision, we base our judgment on objectively accurate external criteria but also on more subjective internal criteria like intrasubject processes or personal preferences for a specific response style or stimulus type etc. (Nakao et al., 2013, 2019; Wolff et al., 2019). Signal detec-

---

tion theory (SDT) distinguishes between objective and more subjective criteria influencing the decision in forced choice tasks (Macmillan and Creelman, 2005). The general assumption of SDT is that decisions are made against a background of uncertainty, e.g., noise (Anderson, 2015); the goal of the decision-maker is to extract the decision signal from such background noise which may lead the participants to introduce a bias in their decisions. This bias is operationalized in SDT by the Criterion C. In contrast, the sensitivity measure d' in SDT is an indicator of the external, objective criteria that indicate the discriminability between the two stimuli by the participant, thus reflecting a measure of accuracy.

While the dorsolateral prefrontal cortex (dlPFC) is known to be implicated in decision making (Reckless et al., 2013; Krain et al., 2006) as it mediates executive function (Dubreuil-Vall et al., 2019), working memory (Balderston et al., 2020) and the self (Frewen et al., 2020), little is known about the neuro-temporal mechanisms underlying Criterion C and Sensitivity d'. Recent studies suggest a link between the Criterion C and spontaneous or ongoing activity like in the pre-stimulus neural activity of monkeys (van Vugt et al., 2018) and humans (Iemi et al., 2017; Iemi and Busch, 2018; Limbach and Corballis, 2016; Samaha et al., 2020). The apparent role of the spontaneous activity in mediating Criterion C suggests that the former's Intrinsic Neural Timescales (INT) (Wolff et al., 2022) may be involved in mediating the cognitive bias. The INT are particularly long in the spontaneous activity of the cortical midline regions of the default-mode network (DMN) which, interestingly, are key regions in mediating self-specificity (Kolvoort et al., 2020; Wolff et al., 2019; Smith et al., 2022). Together, these observations suggest a relationship of INT in CMS/DMN and the dlPFC with the cognitive bias, that is, the Criterion C.

The INT are measured by the autocorrelation window (ACW) through determining the degree to which the brain's activity correlates with itself over time (Wolff et al., 2022; Golesorkhi et al., 2021b; 2021a; Hasson et al., 2015; Honey et al., 2012; Yeshurun et al., 2021). Constituting temporal windows, the INT play an important role in input processing and cognition driven through temporal integration and segregation (Wolff et al., 2022; Yeshurun et al., 2021; Himberger et al., 2018). Temporal integration occurs by temporally smoothing different inputs at different timepoints into one coherent source of information, e.g., summing different words to one sentence through a long INT (Wolff et al., 2022; Himberger et al., 2018). On the other hand, temporal segregation of the external stimuli features is mediated primarily by short ACW in unimodal sensory regions (i.e. primary visual cortex, etc. (Golesorkhi et al., 2021b)). Hence, the length of the ACW can be conceived as a proxy of the balance of temporal segregation and integration (Wolff et al., 2022; Golesorkhi et al., 2021b; 2021a; Himberger et al., 2018). How such balance of temporal integration-segregation through long-short INT/ACW is related to the cognitive bias as measured by the SDT indices (and specifically Criterion C) remains yet unclear, though.

To clarify this relationship, we conducted a combined behavioral, neural, and computational study. Probing the cognitive bias, we used a modified version of a well-established task (Tsakiris, 2008) on visual perception of faces presented in a self-other continuum of different morphed pictures. Given the key importance of timescales with their supposed role in temporal integration-segregation, we presented the task in two temporally distinct ways (Huk et al., 2018). Once we presented it in a discontinuous or discrete way as typical event-related paradigm (separate single faces with different degrees of morphing in order to calculate Criterion C and Sensitivity d' based on the SDT). Additionally, we presented the same task also in a continuous way with an ongoing sequence of morphed faces where the participant had to indicate the transition between the two faces; this allowed us to specifically test for temporal integration-segregation within the paradigm itself, that is on the psychological level. EEG was recorded during both resting state and task-related activity and analysed on both channel and source space regional level. Finally, applying a data-driven network model (Chaudhuri et al., 2015), we included computational modeling to further support the as-

sumption of different processes in CMS/DMN and sensory regions like temporal integration and segregation respectively.

First, we will analyze the behavioral data by extracting the SDT indices and the transitions between self-other faces in both the discontinuous and continuous version of our task. We hypothesize a relation between the discontinuous and the continuous paradigm, that is a correlation between participants' bias (Criterion C) in the discontinuous paradigm with the participants' behavior in the continuous one. Given that the continuous version explicitly probes temporal integration versus segregation, it provides behavioral evidence for the involvement of temporal integration and segregation in the cognitive bias, i.e., Criterion C, and accuracy, i.e., sensitivity d'.

Next, we extract the ACW of EEG resting and task state activity in order to establish its link to the SDT indices. We expect the longer ACW (ACW0) to be implicated in the cognitive bias (Criterion C) while the shorter ACW (ACW5) supposedly mediates discrimination (sensitivity d'). We then also conducted source space reconstruction in EEG. This served to probe whether the cognitive bias, namely Criterion C, is related to the long ACW (ACW0) in the CMS/DMN (as being closely related to the self; (Northoff et al., 2006; Frewen et al., 2020; Qin et al., 2020)) and the dlPFC (as being implicated in decision making;(24, 25)), while the sensitivity d' supposedly is more associated with shorter timescales (ACW5) in sensory regions like primary visual cortex. Does this uni-transmodal hierarchy of ACW play a role in the temporal integration-segregation of inputs? We probed this question by applying the temporal input structure of the empirical-behavioral study in a computational realistic neural network model relying on Chaudhuri et al. (Chaudhuri et al., 2015). This model reinforces the idea that the CMS/DMN's neural activity shows high degrees of temporal integration of distinct inputs across time, while primary visual cortex favors temporal segregation of temporally distinct inputs. Moreover, elimination of the uni-transmodal hierarchy in the computational model abolishes any differences in input processing with regard to different degrees of temporal integration and segregation. That supports the assumption that the long ACW in CMS/DMN with its relation to the cognitive bias (Criterion C) is indeed related to temporal integration, that is, the temporal smoothing of temporally parsed inputs or stimuli across time, along a uni-transmodal hierarchy. Finally, we confirm the specific relationship between ACW and the cognitive bias as a stimulus-unspecific basic decision-making process by investigating the ACW – cognitive bias relationship in the dorsolateral prefrontal cortex (dlPFC), as well as in the fusiform face area specialized for the perception of faces (Kanwisher and Yovel, 2006).

## 2. Methods

### 2.2. Participants

Twenty-seven participants (15 women, 12 men, age: 22.18, SD: 4.28, range: 19 to 36) were recruited. All of them had a current or history of psychiatric or neurological disorders and normal or corrected-to-normal vision. We excluded one participant due to technical problems with EEG recordings in rest and task state and another participant was excluded only for the task state. Participants performed two morphed face recognition tasks adapted from (Tsakiris, 2008): In the discontinuous task, one participant was excluded. In the continuous task, one participant had no behavioural data due to a technical problem. Written informed consent for each participant was obtained prior to study participation. The study was approved by the local Research Ethics Board (REB # 2018054).

### 2.3. Materials

Prior to the experiment, pictures were taken from each of the participants with a Samsung A50 phone. Participants were asked to show

a neutral facial expression, mouth closed. The pictures were then prepared in the free and open-source graphics editor GIMP (2.10.12). All faces were turned to black and white (grayscale) and cut in an oval circle, with only the eyes, nose, and mouth areas remaining on a black background. Then, each face was morphed with a same-sex and same-race face from the NimStim facial pictures set (Tottenham et al., 2009). Morphings were realized with the Abrosoft Fantamorph 5 Software in 1% steps (from 0% self to 100% self-face).

### 2.4. Continuous morphing task (Fig. 1A left)

A hundred and one morphed pictures in 1% morphing steps were extracted from the continuum between the own and the other's face. A control continuum between a famous and an unknown face has also been created, leaving us with four morphing conditions based on the order and the identity depicted on the pictures. The 'self' conditions have the morphing order (Amodeo et al., 2021) from the 'self' face to other face (SO), or from (Barton et al., 2021) other face to 'self' face (OS). The control conditions have a morphing order from a (Nijhof et al., 2020) famous face to an unknown face (FU), or from the (Sparks et al., 2016) unknown face to the famous face (UF). The order of the conditions was randomised.

Pictures were presented in a continuous manner to create the experience of a morphed movie between the two faces. Movie duration was between 10 and 15 s and the interstimulus interval varied between 4 and 6 s. A total of 200 trials, 50 trials per condition in 8 blocks was presented. Participants were instructed to press a key when they stop to see the first face and to give another key when they started to see the second face. Two keypresses are of particular interest as they are the most self-related: In the morphing order from self to other (SO), the first keypress indicates the loss of the own face, while the second keypress in the order from other to self (OS) indicates the emergence or extraction of the own face. In order to record neuronal activity without motor activity noise due to a keypress (Tsuchiya et al., 2015), five trials in each condition were visualized and recorded while no keypress was given (no-report paradigms). The no-report trials took place before the report-trials for the half of participants, and afterwards for the other ones. To ensure that the moment of the keypress was time-independent, we randomly varied the movie length between 10 and 15 s. In addition, the intertrial interval was jittered between 4 and 6 s (jittered by 1 s). This task has been recorded in EEG.

Such a continuous paradigm structure serves the purpose of probing for participants' capacity to integrate or segregate temporally disjointed but sequential inputs, i.e., the morphed self-other faces. Temporally adjacent stimuli like two morphed faces may be temporally integrated/separated entailing separate judgement as self or other; alternatively, they may be integrated entailing subsumption of both under either self or other.

### 2.5. Discontinuous signal detection task (Fig. 1A right)

This task purely served to extract the SDT indices. From the morphed pictures, 13 pictures were selected at a morphing degree from 0% to 100% self in 10% steps. The middle morphing values (40 to 60%) are selected in 5% morphing steps to gather a more fine-grained behavior in the ambiguous range. Each picture was presented 12 times in a random order for 200 ms, with a total 156 trials per participant (Fig. 1A right). Participants were instructed to classify each of the pictures in 'self' pictures (more self than the other) or in 'other' pictures (more other than self). No correct response was possible for the 50% morphing, while morphings above 50% are self-pictures and below 50% are other-pictures. We analysed the data with Signal Detection Theory (SDT) which offers cognitive bias (Criterion C) and sensitivity (d') measures based on the relation of hits and false alarms.

### 2.6. Resting-state

Eyes open resting-state was recorded in EEG for 7 min. The participants were fixating a white cross on a gray background.

## 3. Data analysis

### 3.1. Signal detection theory (SDT)

The discontinuous task was analysed with SDT (Macmillan and Creelman, 2005) because it yields separate indicators for the accuracy in form of the cognitive bias Criterion C and sensitivity d' (Fig. 1B). *3.1.1. Criterion C:* The criterion C of the signal detection theory (Macmillan and Creelman, 2005) indicates the preference of the participant to report rather one than the other of the two faces *when* committing an error (false alarms or misses). It is calculated based on the Hit and False alarm rate as follows (Anderson, 2015):

$$Criterion\ C = -0.5 * \left( z_{Hit} + z_{FA} \right)$$

Some participants tend to indicate perceiving their own face more often than the other's face (liberal response style with a Criterion C > 0), whereas other participants rather see the 'other' face than themselves (conservative response style with a Criterion C < 0). Some participants show no bias (C = 0).

### 3.1.2. Sensitivity d'

d' is a measure of discriminability and indicates the ability of a participant to distinguish between two stimuli. In our case, it indicates how well the participant distinguished between their own and someone else's face. It is calculated based on the hit and false alarm rate (Anderson, 2015).

$$Sensitivity\ d' = z_{Hit} - z_{FA}$$

If the hit rate equals the false alarm rate, d' = 0 where the participant is unable to discriminate between the two stimuli. A higher d' corresponds to less errors and therefore indicates a higher sensitivity towards the differences between two faces.

### 3.2. EEG data acquisition and preprocessing

EEG data was recorded using Ag/AgCl electrodes through a 64-channel Brain Vision Easycap (according to the International 10–20 System) referenced to the right mastoid. The data was sampled at 1,000 Hz with DC recording. The EEG data preprocessing was performed using the EEGLAB toolbox for MATLAB (R2017b; (Delorme and Makeig, 2004), RRID: SCR_007292). The data was downsampled to 500 Hz and filtered with a FIR zero-phase low-pass filter at 50 Hz and a high-pass filter at 1 Hz. With a custom script, noisy channels (defined as 5 interquartile above or below each channels mean) have been spherically interpolated before re-referencing to the average. Further, artifacts were identified using independent component analysis (ICA) via the EEGLAB software (infomax) creating 63 independent components. Next, we used MARA implementation to automatically reject noisy components (Winkler et al., 2011).

### 3.3. Autocorrelation window (ACW)

The autocorrelation function measures the similarity of a time series with a time-lagged version of itself. We distinguished, following Golesorkhi et al. (2021b) and Smith et al. (2022), ACW5 and ACW0. We defined ACW5 and ACW0 as the first lag where the autocorrelation function (ACF) reaches half of its maximum value (AC = 0.5) or zero (AC = 0.0), respectively (Honey et al., 2012; Murray et al., 2014). We calculated both ACW0 and ACW5 to see the impact of longer (ACW0) and shorter (ACW5) windows on the different behavioral indices, i.e., d' and C. Similarly, we further defined ACW4 (AC = 0.4), ACW3 (AC = 0.3),
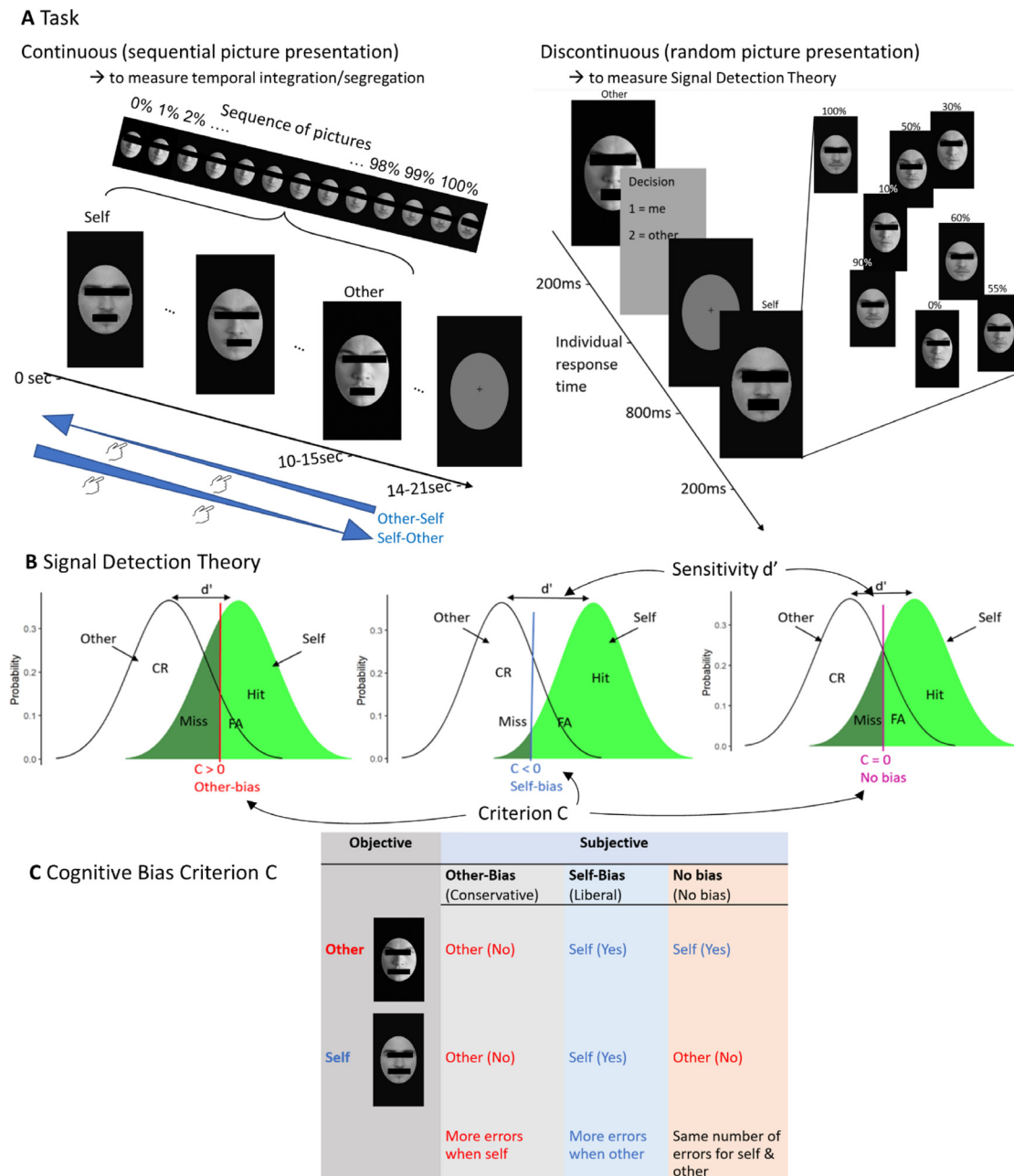
**Fig. 1. A** Procedure of the morphing tasks. In the continuous task (left) morphings of faces were shown in form of a smooth video (ordered sequence of faces). Participants were asked to indicate when they stop to see the first face and when they started to see the second face. Of particular interest are the two self-related keypresses which indicate the loss and the emergence of the own face. On the right is the discontinuous design (right) elaborated to extract Signal detection theory (SDT) indexes. Participants were asked to classify randomly presented morphed faces into 'self' (>50% morphing) or 'other' (<50% morphing) faces. Identities have been made unrecognizable for publication purposes. **B** Schematic description of the SDT. The Sensitivity d' indicates how well a participant discriminates between the two stimulus types 'other' and 'self' faces by indicating the distance between the white (other) and the green (self) curve. The Criterion C indicates a favoritism to one of the two error types miss or false alarm. This indicator will be used to assess the self – and the other bias. **C** Simplified representation of the cognitive bias.

ACW2 (AC = 0.2) and ACW1 (AC = 0.1) to investigate an eventual gradient that links the timescales to the behavioral indices.

All autocorrelations were calculated on 7 min rest and task state EEG data, for each channel (or region of interest (ROI) for eLORETA) before being averaged across all electrodes/ROIs to extract one ACW value per participant.

### 3.4. Source localization with eLORETA

Regions were defined according to the Glasser parcellations (Glasser et al., 2016). Exact Low Resolution Electromagnetic Tomog-

raphy (eLORETA (Pascual-Marqui et al., 1994)) was performed by estimating the virtual-channel source for each region of the Glasser atlas in FieldTrip (Oostenveld et al., 2011). The output is a timeseries of estimated source level activity for each region. We investigated the core DMN (Andrews-Hanna et al., 2014) consisting of the posterior cingulate cortex (PCC) and the pregenual anterior cingulate cortex (pACC) because of its known implication in self-related functioning. As a control region not specifically implicated in self-related processing, we choose the visual primary cortex (V1). We investigated the dorsolateral prefrontal cortex (dlPFC) because of its implication in decision making and the FFA due to its implication in face processing. The precise Glasser-

parcels used were the following: V1: LV1, RV1. CMS/DMN: LRSC, RRSC, L23d, R23d, Ld23ab, Rd23ab, L23c, R23c, Rp24, Lp24, Ra24, La24, L31a, R31a, L31pv, R31pv. dlPFC: L8C, R8C, L8Av, R8Av, Li68, Ri68, LSFL, RSFL, L8BL, R8BL, L9p, R9p, L9a, R9a, L8Ad, R8Ad, Lp946v, Rp946v, La946v, Ra946v, L46, R46, L946d, R946d. Fusiform face complex: LFFC, RFFC.

### 3.5. Statistical analyses

Comparisons of the ACW based on the thresholds were performed via a repeated measures ANOVA with a Greenhouse-Geisser correction for sphericity violations. The link between the behavioral and neuronal measures was obtained via simple Pearson's correlations. For the mathematical models describing the gradient between ACW and the behavioral variables, the ACW0 was replaced by 0.01 for logarithmic transformation. The remaining ACW values are their AC value (e.g., 0.1 for ACW1, 0.2 for ACW2 etc.). Inferential analyses were run in JASP or R. ACW was extracted in Python (3.8). SDT indices were calculated in Excel following the instructions in (Macmillan and Creelman, 2005).

### 3.6. Computational model

To further probe the effect of different regions on temporal segregation and integration, we used a computational model based on (Chaudhuri et al., 2015). In essence, this model comprises two differential equations:

$$\tau_E \frac{d}{dt} v_E^i = -v_E^i + \beta_E \Big[ \big(1 + \eta h_i\big) \Big( w_{EE} v_E^i + \mu_{EE} \Sigma_{j=1}^N FLN_{ij} v_E^j \Big) \\ - w_{EI} v_I^i + I_{ext,E}^i \Big]_+$$

$$\tau_I \frac{d}{dt} v_I^i = -v_I^i + \beta_I \Big[ \big(1 + \eta h_i\big) \Big( w_{IE} v_E^i + \mu_{IE} \Sigma_{j=1}^N FLN_{ij} v_E^j \Big) \\ - w_{II} v_I^i + I_{ext,I}^i \Big]_+$$

$v$ is the firing rate, $\tau$ is the intrinsic time constant, $I_{Ext}$ is the external input to the system governed by the slope b of the f-I curve. $w$ values are coupling parameters. m is a fixed parameter that controls the strength of long-range excitatory input. FLN (Fraction of Labeled Neurons) is the structural connectivity matrix based on a macaque study (Markov et al., 2014). E and I correspond to excitatory and inhibitory, respectively; $i$ and $j$ denote different regions. Solving these differential equations gives us 29 time series, one per region in the model. We used the exact same parameters as (Chaudhuri et al., 2015). The hierarchy index $h$ is a sigmoid function scaled between 0 and 1, increasing from periphery to core. First, we used a continuous input of 1 s and plotted activity the same way. We also simulated the input as close as the real discontinuous paradigm in this study. We gave 200 ms inputs with amplitude 1 to the outermost region (V1) and randomized the inter-stimulus interval (ISI) between the mean of the ISI in the study (0.528 s) +−1SD (0.253 s) and plotted the resulting neural activity changes in both periphery (V1) and core (24c) regions. In a second step, to probe the effect of the hierarchical uni-transmodal topography on temporal segregation and integration, we eliminated the hierarchy by setting the hierarchical index $h$ to 0.5 for all regions.

## 4. Results

### 4.1. Behavioral results

In the discontinuous self-task (Fig. 1A right, see Methods), participants indicated the predominant facial identity (self or other) of single randomly presented morphed faces reflecting an event-related paradigm structure. The psychometric function (Fig. 2B) indicating the proportion

of correct classifications for each morphing degree shows more variability in the middle morphings (where the subjective uncertainty is higher) than in the extreme ones (where the subjective uncertainty is lower). The Sensitivity index d' had a mean (SD) of 2.65(0.52) (range: 1.6 to 3.79). The cognitive bias Criterion C had a mean (SD) of 0.25 (0.5) (range: −0.51 to 1.34).

Next, for each participant, we calculated the average of the morphing degree at the moment a keypress was given. The descriptive results are as follows: Loss of self: $m = 50.77$, SD = 7.88, range = 30.27, max = 60.33, min = 30.06; Emergence of other: $m = 75.789$, SD = 7.001, range = 28.31, max = 88.74, min = 60.43; Loss of other: $m = 46.59$, SD = 7.19, range = 24.38, max = 60.49, min = 36.11; Emergence of self: $m = 71.8$, SD = 8.33, range = 31.75, min = 54.86, max = 86.61; Fig. S1). The simultaneous effect revealed by a repeated ANOVA is significant (F(3,75) = 104.467, $p < .001$, $h^2_{patial} = 0.807$; $e_{GG} = 0.697$), post hoc differences are reported in Fig. S1. We observe no effect specific to the order of morphing presentation (SO or OS).

Due to our particular interest in the self, we will specifically focus on its loss and its emergence (as obtained by the continuous task). Hence, we correlated these two keypresses with C and d' (as obtained in the discontinuous task). We see that only the keypress related to the emergence of the self correlated with the Criterion C ($r = 0.486$, $p = 0.014$, Loss: $r = −.275$; $p = .215$; Fig. 2C) but not with the sensitivity d' (Emergence: $r = 0.150$, $p = .474$; Loss: $r = −.299$, $p = .147$). This indicates that an early detection of the own face is linked to a liberal self-bias. A later self-emergence is linked to a conservative 'other'-bias.

### 4.2. Intrinsic neural time scales in rest and task states

We assessed the intrinsic neural timescales (INT) by the autocorrelation window (ACW; Fig. 3A). We investigated the topographic maps of ACW (Fig. 3B) which show the expected rostro-caudal gradient (Golesorkhi et al., 2021b, 2021a; Kiebel et al., 2008) and observe an overall significantly longer ACW during task compared to rest (Fig. 3C), indicating a sensitivity of the ACW to external stimuli.

### 4.3. Relationship of intrinsic neural timescales with behavioral measures

First, we identify the correlational strength between the different behavioral measures (Emergence of Self, Criterion C, Sensitivity d') with the ACW via Pearson's correlations (Table S2a to Table S3b). Next, we investigated the relationship between these different correlations via different mathematical functions (Fig. 4, for more details see Table S4). In resting state, the correlation between the moment of the Emergence of Self is strongest for ACW0 and decays following a logarithmic function ($p = 0.003$). We observe the same evolution for the Criterion C ($p = 0.014$). Inversely, an increasing logarithmic function links the d' to the ACW ($p = 0.0003$), with the strongest correlation observed for ACW5. In task state, the relationship of ACW with the Emergence of Self and Criterion C can be described via a quadratic function ($p = 0.007$ and $p = 0.009$, respectively). This link is lost (due to one data point) for sensitivity d' ($p = 0.1$). By taking the difference between rest and task state, we confirm the differential correlation gradient between Criterion C and d' and confirm the similarity between the Emergence of Self and Criterion C: The rest-task difference of Emergence of Self and Criterion C follows a quadratic function ($p = 0.023$ and $p = 0.011$, respectively), while the rest-task difference of Sensitivity d' shows a simple linear relationship ($p = 0.0003$). No coherent relationship links the ACW to the Loss of self (Fig. S2).

### 4.4. Source space reconstruction eLORETA in CMS/DMN and V1

We extracted regional activity via eLORETA for the DMN focusing on CMS/DMN (PCC and pACC) and the primary visual area (V1; see Methods). ACW was calculated on the extracted DMN regions and correlated with d' and Criterion C (Table 1). The Criterion C is only associated
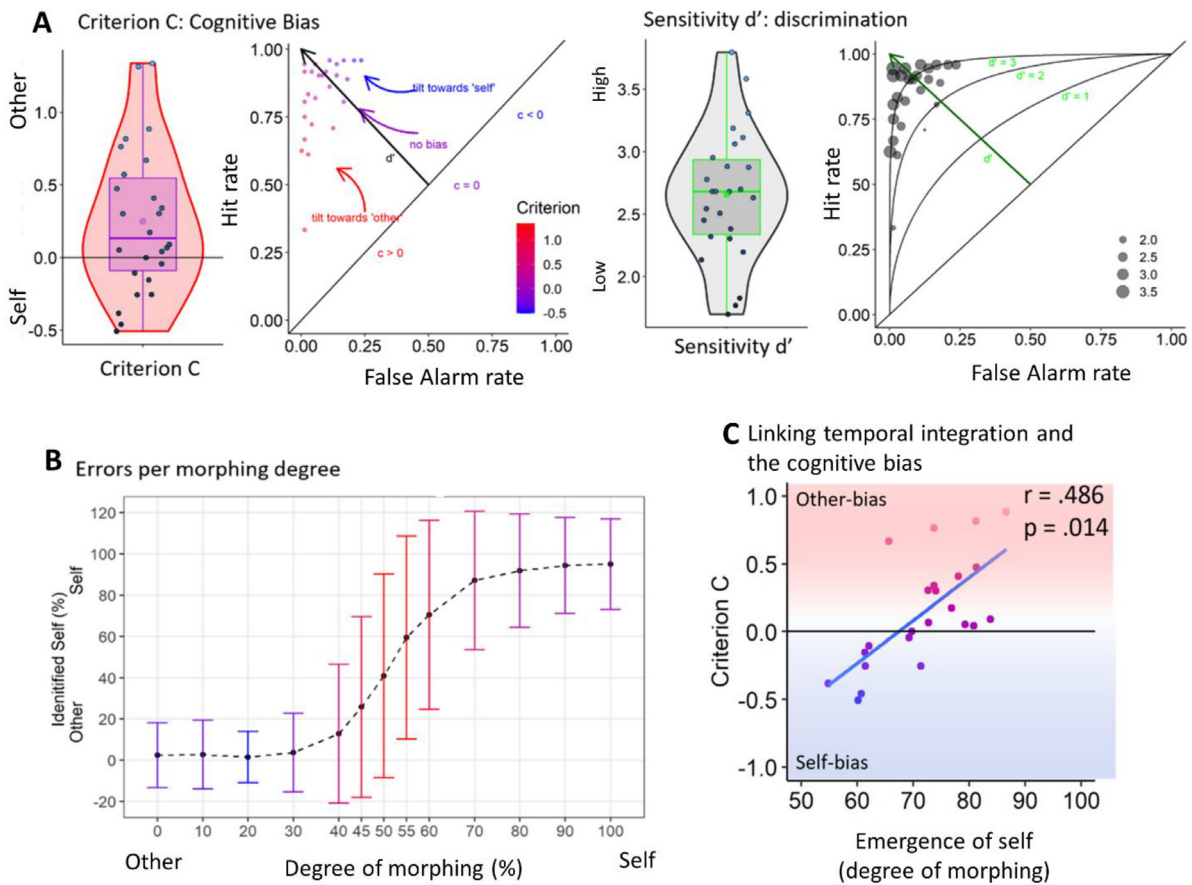
**Fig. 2. A** Sensitivity d' and Criterion C extracted based on the discontinuous task. Descriptive data of the d' (left) and Criterion C (right) in a violin plot and a ROC space. **B** Psychometric function of the participant's responses to the different morphing degrees in terms of identified self (error bars indicate SD) **C** The strong correlation of the Criterion C and the Emergence of self keypress indicates that an early detection of the own face is linked to a self-bias. A later self-emergence is linked to an 'other'-bias.

**Table 1**
Correlations between Criterion C (Crit C) and Sensitivity d' (Sens d') in the DMN and the primary visual area V1 via the ACW0 (_0) and ACW5 (_5).

| | | Crit C | | Sens d' | |
|---|---|---|---|---|---|
| | State | r | p | r | p |
| DMN_0 | rest | 0.342 | 0.094 | 0.207 | 0.321 |
| | task | 0.502* | 0.012 | 0.188 | 0.38 |
| DMN_5 | rest | 0.308 | 0.143 | 0.339 | 0.106 |
| | task | 0.251 | 0.238 | 0.242 | 0.254 |
| V1_0 | rest | −0.043 | 0.838 | 0.007 | 0.973 |
| | task | 0.387 | 0.062 | 0.11 | 0.608 |
| V1_5 | rest | 0.071 | 0.735 | 0.469* | 0.018 |
| | task | 0.283 | 0.191 | 0.306 | 0.155 |

with the ACW0 in the DMN, measured during task-state (DMN-ACW0: $r = 0.502$, $p = 0.012$, Fig. 5A). Neither the V1 nor the ACW5 elicited a significant correlation with the Criterion C ($p > .05$). The Sensitivity index d' is only correlated with the ACW5 in the resting state V1 activity (V1-ACW5: $r = 0.469$, $p = .018$, Fig. 5A). Neither the DMN nor the ACW0 showed significant correlation with the d' ($p > .05$).

### 4.5. Computational modeling – temporal integration and segregation in CMS and sensory cortex

The hierarchy of different regions in the model was defined by a sigmoid function scaled between 0 and 1 (see methods). First, we applied the continuous task paradigm on the model to probe temporal segregation in hierarchically low regions (periphery / V1) and integration in

hierarchically high regions (core / 24c; Fig. 6, left column). In a second step, in order to investigate the effect of the differential hierarchical positions of visual cortex and CMS/DMN in their short and long timescales, we eliminated the hierarchy in our computational model by assigning the same hierarchical index to all regions. We now observed similar activity in both V1 and midline 24c (Fig. 6, right column).

### 4.6. ACW mediates the bias in decision making in a stimulus-unspecific rather than -specific way

In a next step, we wish to investigate if the link between the cognitive bias and the ACW is mediated by the process of decision making itself operating across different types of stimuli, e.g. stimulus-unspecific, rather than by the content of the facial stimuli (self vs. other vs. famous vs. unknown), e.g., stimulus-specific. For this, we will first confirm the link between the long ACW and the cognitive bias in the dlPFC. Hence, we extracted the ACW of the dlPFC and found a correlation between the ACW0 in the dlPFC only with the Criterion C in rest ($r = 0.485$, $p = 0.014$) and task ($r = 0.530$, $p = 0.008$, Fig. 7). This confirms the intimate link between the long ACW and the cognitive bias in our decisions and supports the association of ACW with the decision-making process itself. The short ACW5 of the dlPFC is exclusively linked to the Sensitivity d' in rest ($r = 0.420$, $p = 0.036$, Fig. 7; Table S5), confirming the link between the short ACW and sensitivity d' in the accuracy of decision making.

In a second step, we extracted the ACW during the visualization of each face identity (self, other famous, unknown). A repeated measures ANOVA shows no significant differences in the ACW between the facial
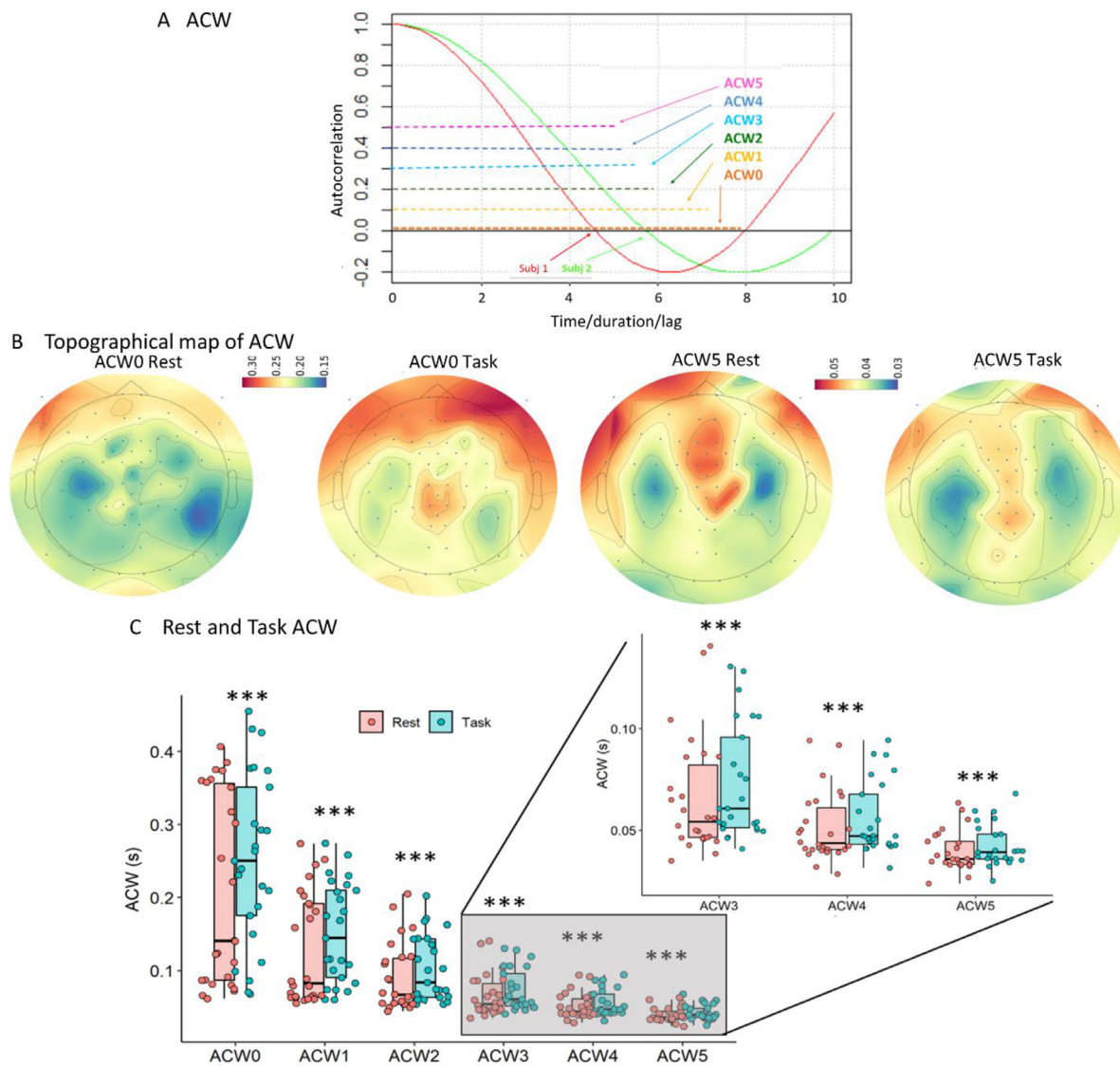
**Fig. 3.** **A** Autocorrelation Window (ACW) of two schematic participants (green and red). Indicated are the six degrees of AC (in color from pink to orange) on the y-axis, and the duration on the x-axis. The ACW is the lag until a certain correlation value within the overall autocorrelation function is reached. We observe the expected rostro-caudal gradient of ACWs. **B** Topographical maps of the ACW0 and ACW5 in rest and task state averaged across participants. **C** Boxplots of all six ACWs averaged across participants and EEG-channels show a clear rest-task differences.

identity (ACW0: $F(3,72) = 1.207$, $p = 0.313$; ACW5: $F(3,72) = 0.282$, $p = 0.838$; see Fig. S3), indicating a certain insensitivity of the ACW towards the stimuli content.

We then correlated the ACW of the different facial stimuli with the Criterion C and Sensitivity d'. The ACW0 extracted from each face correlated with the Criterion C ($p < .5$; Table S6), confirming an insensitivity of the ACW towards the facial identity or the stimulus content in relation to the cognitive bias.

Finally, we calculated the ACW on activity extracted from the fusiform face area (FFA) and correlated it with the SDT measures. No significant correlations were found ($p > .05$; Table S7), indicating that the FFA is not mediating the link between cognitive bias and ACW. Together, these findings strongly indicate the stimulus-unspecific effects of ACW on the bias in decision making.

## 5. Discussion

In the present study, we investigated whether temporal integration mediates the cognitive bias of self in perception and decision making.

For this, we combined behavioral, neural and computational levels of analyses. Using Signal Detection Theory (SDT), we observed the cognitive bias on the behavioral level (Criterion C) with different participants showing bias towards either the own or other face. Given the nature of our paradigm, this implies high temporal integration on the psychological level. This was further extended to the neural level by showing that the cognitive bias is specifically associated with longer INT (ACW0) in CMS/DMN and dlPFC, thus suggesting high temporal integration on the neural level. This is complemented by computational neural network modeling showing high degrees of temporal integration of temporally distinct inputs in specifically CMS/DMN as distinct from visual cortex, suggesting a strong implication of the uni-transmodal hierarchical topography in the cognitive bias.

### 5.1. Behavioral analyses

First, we observed a strong correlation between the cognitive bias and the keypress indicating the emergence of the own face. This indicates that an early detection of the own face is linked to a liberal self-
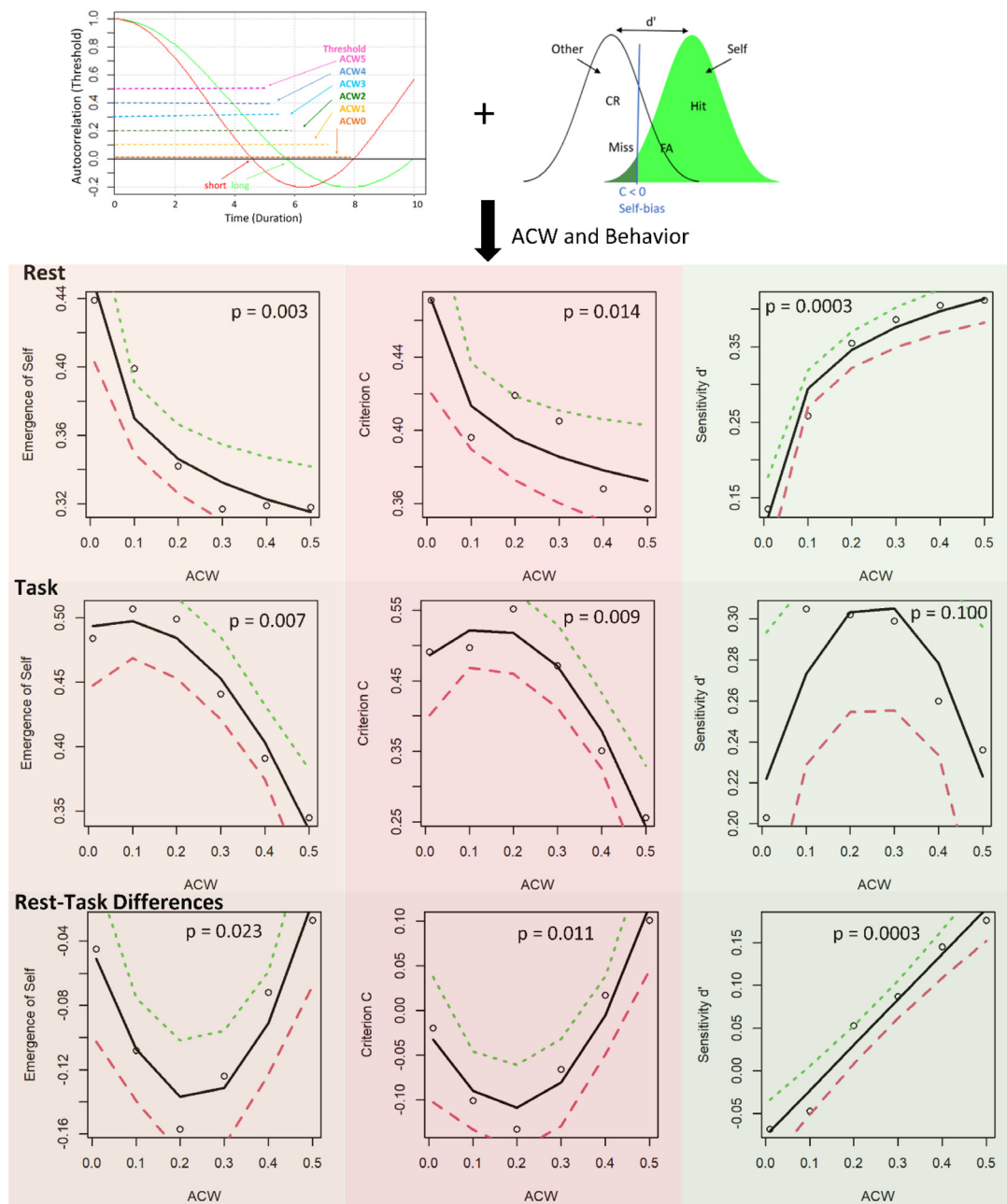
**Fig. 4.** Relationship between the neuronal and behavioral measures. Each column represents one behavioral measure (left: Emergence of self; middle: Criterion C; right: Sensitivity d'). In resting state (upper), task state (middle) and the rest-task difference (lower). The ACW thresholds (e.g., 0.5 for ACW5) are on the x-axis. The y-axis shows the Pearson's correlation coefficient between the behavioral variable and the different ACWs. In resting state, the curves show a decreasing logarithmic evolution for the Emergence of Self and Criterion C but an increasing logarithmic evolution for d'. Similarly in task state, Criterion C and the Emergence of Self show a quadratic function, which is non-significant in the d'. Finally, rest-task differences confirm the differential relationship between the ACW with Criterion C and Emergence vs. ACW with d': For Criterion C or the Emergence, we find stronger correlation with the longer ACW0, while the d' is strongly linked to the shorter ACW5.

bias. A later emergence is linked to a conservative 'other'-bias. Together, these findings strongly support that temporal integration is a key factor in mediating the bias Criterion C. We will next demonstrate the key role of temporal integration in the cognitive bias by investigating the ACW.

### 5.2. Intrinsic neural timescales

Employing the different ACWs enabled us to investigate a more fine-grained temporal resolution. A shorter ACW can be observed in primary sensory areas like the temporal and occipital channels while a longer ACW is mostly observed in parietal and frontal channels. We expect

shorter temporal windows (i.e., ACW5) to represent stronger degrees of temporal segregation while the long temporal windows of ACW (i.e. ACW0) are more related to high degrees of temporal integration. We observe an overall significantly longer ACW during task compared to rest (Fig. 3C), indicating a sensitivity of the ACW to external stimuli. This is well in accordance with its supposed role in input processing (Smith et al., 2022; Golesorkhi et al., 2021b, 2021a; Zilio et al., 2021). A longer ACW in task than in rest seems to be related to continuous paradigms which demand stronger temporal integration, while shorter ACW in task than in rest are found in event related paradigms which are demanding in temporal segregation (Wolff et al., 2022; Smith et al.,
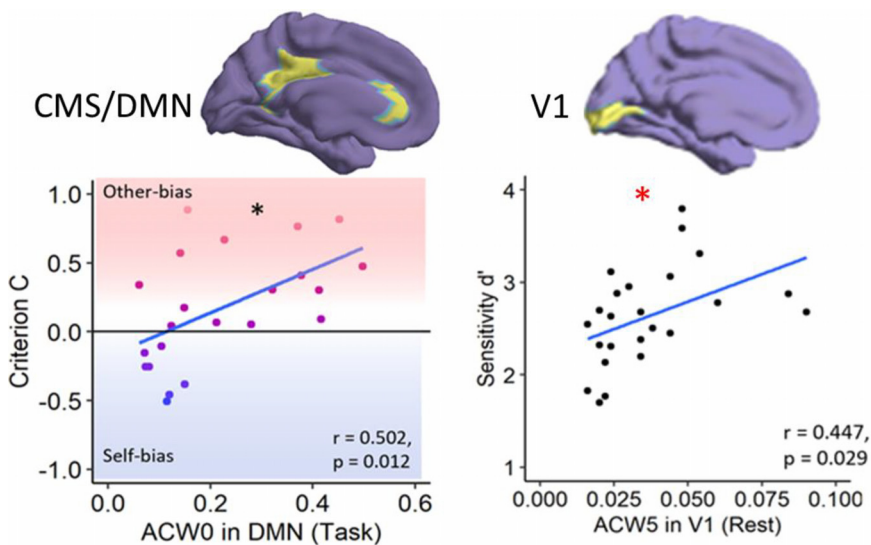
**Fig. 5. A** Linking the Sensitivity d' and Criterion C to the cerebral regions via the ACW. The Criterion C is correlated with the eLORETA CMS/DMN activity while the Sensitivity d' correlated with the V1 activity. A long ACW0 is linked to an other-bias, while a shorter one is associated to an self-bias. A longer ACW5 is linked to a better performance (d').

2022). Further, rest and task correlate highly (*r* > 0.85) with each other (Table S1), indicating a strongly shared or common neural basis between rest and task confirming previous data (see Smith et al., 2022; Golesorkhi et al., 2021b)).

### 5.3. Relationship of intrinsic neural timescales with behavioral measures

To demonstrate the implication of temporal integration and segregation on a psychological level, we investigate the link between the behavioral measures (self-related keypresses, d' and Criterion C) and ACW (which is an indicator of temporal integration and segregation on the neural level (Wolff et al., 2022)). Given that both, perception-based Criterion C (van Vugt et al., 2018; Iemi et al., 2017; Iemi and Busch, 2018; Limbach and Corballis, 2016; Samaha et al., 2020) and self-consciousness (Qin and Northoff, 2011; Wolff et al., 2019; Davey et al., 2016; Huang et al., 2016), have been associated with the brain's spontaneous activity, we associated the behavioral variables with both, rest – and task-related ACW.

Firstly, the Emergence of Self is strongly correlated with the longer ACW (ACW0), indicative of a higher degree of temporal integration. This confirms the integrative nature of the continuous task and shows that it is the emergence, not the loss of the self, that is specifically linked to temporal integration and long ACW (Kolvoort et al., 2020; Wolff et al., 2019; Smith et al., 2022). It is to notice that an antagonistic logarithmic function describes the association between Criterion C and Sensitivity d' to the ACW in resting state. While in task state, behavioral and neural variables are linked via a quadratic function. The rest-task difference confirms the differential role of short and long INT in Criterion C and Sensitivity d', respectively.

Together, these findings support the assumption that the Criterion C is related to higher degrees of temporal integration due to its link to longer ACW. The longer ACW increases the tendency of temporal smoothing and thus lumping together temporally disjointed inputs like the morphed faces. In result of its link to shorter ACW, sensitivity d' is more linked to temporal segregation and the increased capacity to discriminate between sequential faces in a temporally precise way.

### 5.4. Neuroanatomical grounds

The differentiated implications of the ACW in the cognitive indices is further supported and extended on neuroanatomical grounds. The self is known to be closely associated with the cortical midline structures (CMS) like anterior and posterior cingulate cortex of the default-mode network (DMN) (Northoff et al., 2006; Frewen et al., 2020; Qin et al.,

2020; Northoff, 2016) while the dlPFC is known for its role in decision making. Moreover, the core regions CMS/DMN and dlPF in general are known to exhibit the longest ACW compared to primary sensory regions (Qin and Northoff, 2011; Wolff et al., 2022; Golesorkhi et al., 2021b, 2021a; Ito et al., 2020; Raut et al., 2020). Spontaneous activity (Buzsáki, 2006) as for instance pre-stimulus activity in these regions predict the subsequent judgement of stimuli as self-related (Qin et al., 2016). Our data extend these results by showing that the spontaneous and task-related activity in these regions mediate the cognitive bias through long INT (ACW0) and temporal integration.

How is our main finding (longer ACW (ACW0) linked to Criterion C and shorter ACW (ACW5) linked to Sensitivity d') represented in the DMN/dlPFC and the primary sensory regions? In other words, are the Criterion C and the d' modulated by the long and short ACW in DMN/dlPFC and primary visual area? Using eLORETA source space reconstruction, we observed a similar link of the cognitive bias (Criterion C) with the ACW0 and of the ACW5 with the d'. The topographical specifications through eLORETA show that the cognitive bias Criterion C is linked to the DMN and the dlPFC, while the discriminability d' is more related to the dlPFC and the primary visual area.

Together, these results confirm the specific link of the longer ACW0 in the DMN/dlPFC and Criterion C while the shorter ACW5 in dlpFC and V1 relates to Sensitivity d' (Golesorkhi et al., 2021b, 2021a; Chaudhuri et al., 2015). This supports a special role of CMS/DMN and dlPFC in mediating specifically higher degrees of temporal integration (Golesorkhi et al., 2021b, 2021a; Chaudhuri et al., 2015) underlying the cognitive bias in visual perception and subsequent decision making. The Sensitivity d' instead is linked to the shorter timescales (ACW5) of the dlPFC and the primary visual area favouring temporal segregation over integration. Importantly, the Criterion C is an indicator of a continuum between the self- and the other bias.

We observed that a self-bias is linked to short ACW0, while long ACW0 are associated with an other-bias. This is in line with the findings by Smith et al. (2022) who, in a different paradigm, demonstrate that ACW0 is associated with self-related processing. Moreover, Northoff et al. (2021) demonstrate that an abnormally long ACW is related to the basic self-disturbance in schizophrenia. Together, these findings support the key role of especially the longer ACW (ACW0) for mediating the bias, e.g., Criterion C, including self-bias or self-specificity as distinguished from the shorter ACW (ACW5) which mediates accuracy (d').

Is the ACW a stimulus-specific indicator of the facial identity presented in the stimuli (self vs. other vs. famous vs. unknown) rather than being part of the decision processes itself operating in a stimulus-
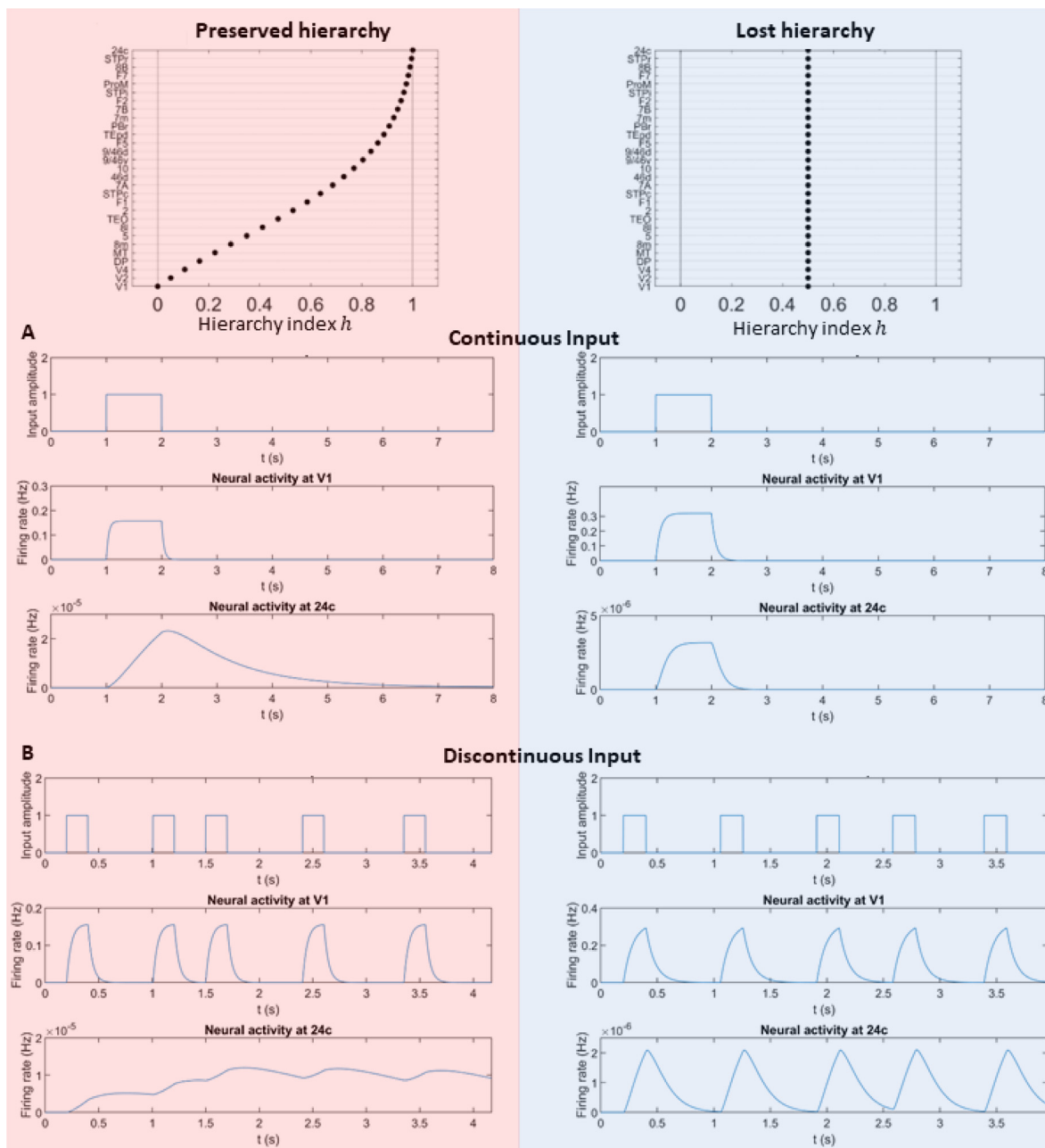
**Fig. 6.** Computational modeling of input processing. Top row depicts the hierarchical structure which scales the effect of local and long-range activity (left) vs. the absence of this hierarchy (right). **A** Continuous task paradigm: When a hierarchy of intrinsic neural timescales apply, the input leads to an extended and expanded neural activity in 24c, whereas it is more or less of the same duration in V1 (left). The elimination of hierarchy renders both regions the same (right). **B** Discontinuous task paradigm: Similarly to the continuous task, the neural activity of the peripheral region V1 shows temporal segregation whereas the core region 24c predominantly integrates different inputs (left). The elimination of hierarchy gives us very similar input processing in both V1 and 24c (right).

unspecific way? To answer this question we correlated the ACW of the fusiform face area (FFA), known by its role in facial processing (Kanwisher and Yovel, 2006) with Criterion C and Sensitivity d'. No link between the SDT measures and the ACW in the FFA was found. Further, we extracted the ACW during the visualization of each face identity (self, other famous, unknown) and no significant difference between them has been shown.

Together, these results show that the ACW mediates the cognitive bias on a basic stimulus-unspecific neuronal level of the decision making itself operating across the different facial stimuli. This supports our assumption that the ACW mediates the stimulus-unspecific temporal processing of all stimuli by providing a temporal envelop for them which,

as per our results, shapes our decision-making process featured by cognitive bias and sensitivity d'.

### 5.5. Computational mechanisms

The large-scale computational model of the dynamical hierarchy of timescales (Chaudhuri et al., 2015) gave us the possibility to probe the effect of different timescales on input processing in our specific task structure (continuous and discontinuous paradigms). Based on our eLORETA results, we were particularly interested to probe temporal segregation in hierarchically low regions (periphery / V1) and integration in hierarchically high regions (core / 24c). Our findings emphasize
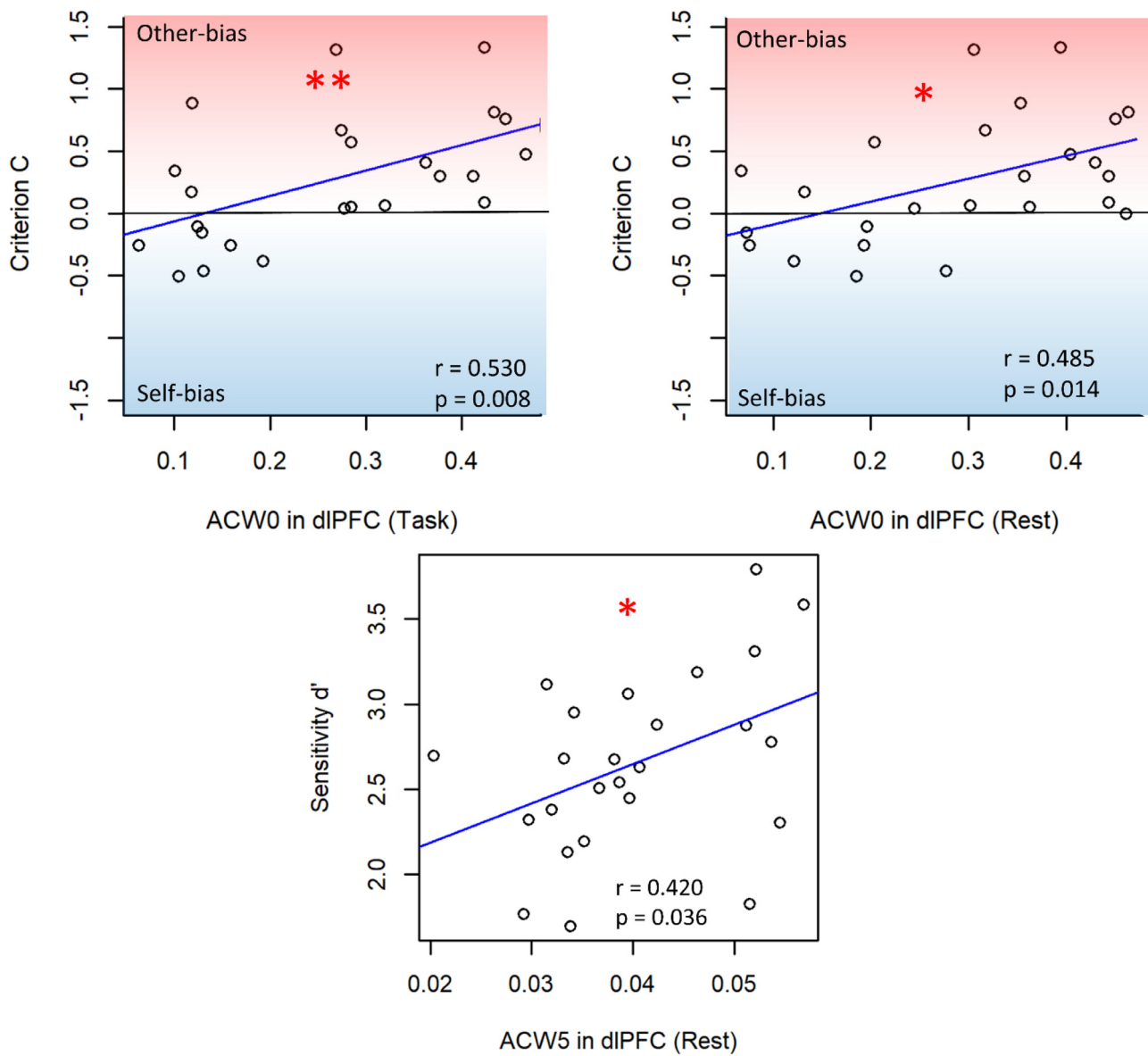
**Fig. 7.** Correlation between the ACW in the dlPFC with the cognitive bias (upper) and sensitivity d' (lower). A long ACW0 is linked to an other-bias, while a shorter one is associated to a self-bias. A longer ACW5 is linked to a better performance (d').

that the temporal hierarchy proposed by Chaudhuri pertains in our task structure. This confirms the implication of temporal segregation in sensory regions like V1 in the processing of disjoint external inputs in a temporally (and objectively) accurate way, related to the sensitivity. On the other hand, the cortical midline region 24c integrates different temporally disjoint inputs along with baseline activity which was shown to be related to self, thus showing a high degree of temporal integration and self bias.

Once we eliminated the hierarchy in our computational model by assigning the same hierarchical index to all regions, we now observed similar activity in both V1 and midline 24c. This suggests that the different degrees of temporal integration and segregation as well as extension during input processing in unimodal regions like V1 and transmodal midline regions like 24c are, at least in part, related to their differential hierarchical positions in the brain's overall uni-transmodal topography. Temporal integration-segregation may thus be an intrinsic feature of the brain's uni-transmodal topography rather than being primarily related to the extrinsic or external input of the paradigm; for that reason, it may remain independent of the specific task, e.g., task-unspecific. Given

that these differential phenomena of temporal integration and segregation in uni- and transmodal regions disappear when abolishing the hierarchy in our model, we suppose, albeit tentatively, a key role of the brain's uni-transmodal topographic organization in mediating the cognitive bias (Criterion C) through the INT.

*5.7. Limitations*

One potential limitation of our study is the novel use of ACW0 as distinct from ACW5 including their association with distinct cognitive features, namely sensitivity d' and Criterion C. However, two previous studies (Smith et al., 2022;Golesorkhi et al., 2021b) also demonstrated differential association of ACW5 and ACW0 with neural, e.g., topographic distinction of transmodal DMN vs unimodal sensory regions, and psychological, e.g., self-continuity, features. This is well in line with our observation of especially the longer variant (ACW0) in trans-modal CMS/DMN being associated with Criterion C.

Yet another potential issue in our study concerns temporal integration. While especially the longer variant, ACW0, strongly suggests high

degrees of temporal integration (Wolff et al., 2022), we did not show it in a more direct way in our empirical EEG data. However, various indirect lines strongly suggest temporal integration to be the main mechanism. First, especially the continuous version of our paradigm with the sequential self-other face morphing required temporal integration and segregation: if two sequential faces are associated with one and the same person, e.g., self or other, the two temporally distinct inputs (or stimuli/faces) must be integrated across their distinct time points. If, in contrast, they are attributed to distinct persons, e.g., self and other, they must be segregated. Temporal integration is thus required on the psychological level of the paradigm itself. Second, we demonstrate temporal integration on the computational level in our simulation where CMS/DMN, unlike visual cortex, do indeed integrate temporally parsed inputs into one activity change.

Additionally, we would like to mention that the CMS/DMN is known to be recruited in self-processing but that the association with this region does not necessarily engender self-specific processing (Frewen et al., 2020). Further studies would be necessary to confirm this link and to extend the knowledge to probe for self-relatedness in our own study.

One may wonder why a majority of participants present an other-bias instead of a self-bias, as per self-prioritization effect. We have to consider that our task is primarily a task about bias in decision making with subjects being forced (due to the morphed nature of the faces) to make mistakes as measured by the Criterion C. This has been described as self-related processing (Northoff et al., 2006; Northoff, 2016). Within that given framework, the bias or error can occur either with respect to other or self which is described as self-referential processing or self-prioritiziation (Sui and Humphreys, 2015). Our study and its paradigm operate primarily on the first level, the level of self-related processing as operationalized by the Criterion C, the bias, rather than on the second level of self-referential processing (as the typical trait adjective tasks). Therefore, we do not see our results in contradiction to the self-reference effects as that operates on the level of self-referential processing rather than self-related processing as target in our study.

Finally, we demonstrate the importance of topographic hierarchy for temporal integration. That, however, was shown only in an indirect way, that is, by abolishing the uni-transmodal hierarchy in our computational model. Future studies in for instance patients with CMS/DMN lesions are warranted that relate different degrees of uni-transmodal topographic hierarchy with different degrees of both temporal integration and cognitive bias.

## 6. Conclusion

In conclusion, we demonstrate the key role of temporal integration for our cognitive bias in perception and decision making. We demonstrate temporal integration on the behavioral level using signal detection theory that allows distinguishing Criterion C (bias) and sensitivity d' (accuracy). This is complemented on the neural level by showing that the cognitive bias is related to longer INT (ACW0) of especially the CMS/DMN and dlPFC. The involvement of temporal integration and the uni-transmodal topography is substantiated by computational modeling showing high degrees of temporal integration of temporally parsed inputs in the neural response of specifically transmodal CMS/DMN and dlPFC (as distinct from unimodal primary visual cortex). Together, we demonstrate that the cognitive bias in perception and decision making is intimately linked to the intrinsic neural timescales as based on the brain's uni-transmodal topographical organization.

## Significance statement

Every day humans take decisions which are frequently characterized by a cognitive bias. We demonstrate the key role of temporal integration in this bias in perception and decision making on a behavioral level using signal detection theory. Neurally, the cognitive self-bias is related to longer Intrinsic Neural Timescales of especially the cortical midline

structures (CMS) of the default mode network (DMN). The involvement of temporal integration in CMS/DMN is further substantiated by computational modeling showing high degrees of temporal integration of temporally parsed inputs in the neural response of specifically CMS/DMN (as distinct from primary visual cortex). Together, we demonstrate that the cognitive bias in perception and decision making is intimately linked to the longer intrinsic neural timescales in core regions.

## Declaration of Competing Interest

The authors declare no conflicts of interest.

## Credit authorship contribution statement

**Angelika Wolman:** Methodology, Software, Validation, Formal analysis, Investigation, Resources, Writing – original draft, Writing – review & editing, Visualization. **Yasir Çatal:** Software, Formal analysis, Writing – original draft, Writing – review & editing, Visualization. **Annemarie Wolff:** Resources, Software, Validation, Writing – review & editing. **Soren Wainio-Theberge:** Software, Writing – review & editing. **Andrea Scalabrini:** Methodology, Validation, Writing – review & editing. **Abdessadek El Ahmadi:** Software, Formal analysis, Validation, Writing – review & editing. **Georg Northoff:** Methodology, Validation, Conceptualization, Writing – original draft, Writing – review & editing, Visualization, Supervision, Project administration, Funding acquisition.

## Data Availability

Data will be made available on request.

## Acknowledgment

## Supplementary materials

Supplementary material associated with this article can be found, in the online version, at doi:10.1016/j.neuroimage.2023.119896.

## References

Amodeo, L., W.iersema, J.R., Brass, M., N.ijhof, A.D., 2021. A comparison of self-bias measures across cognitive domains. BMC Psychol. 9, 132.

A.nderson, N.D., 2015. Teaching signal detection theory with pseudoscience. Front. Psychol. 6.

A.ndrews-Hanna, J.R., Smallwood, J., S.preng, R.N., 2014. The default network and self–generated thought: component processes, dynamic control, and clinical relevance: the brain's default network. Ann. N. Y. Acad. Sci. 1316, 29–52.

B.alderston, N.L., et al., 2020. Patients with anxiety disorders rely on bilateral dlPFC activation during verbal working memory. Soc. Cogn. Affect. Neurosci. 15, 1288–1298.

Barton, T., C.onstable, M.D., Sparks, S., Kritikos, A., 2021. Self-bias effect: movement initiation to self-owned property is speeded for both approach and avoidance actions. Psychol. Res. 85, 1391–1406.

Buzsáki, G., 2006. Rhythms of the Brain. Oxford University Press 10.1093/acprof:oso/9780195301069.001.0001May 27, 2022.

Chaudhuri, R., Knoblauch, K., Gariel, M.-A., Kennedy, H., Wang, X.J., 2015. A large-scale circuit mechanism for hierarchical dynamical processing in the primate cortex. Neuron 88, 419–431.

Christoff, K., Cosmelli, D., Legrand, D., Thompson, E., 2011. Specifying the self for cognitive neuroscience. Trends Cogn. Sci. 15, 104–112.

C.unningham, S.J., T.urk, D.J., 2017. Editorial: a review of self-processing biases in cognition. Q. J. Exp. Psychol. 70, 987–995.

D.avey, C.G., Pujol, J., H.arrison, B.J., 2016. Mapping the self in the brain's default mode network. Neuroimage 132, 390–397.

Delorme, A., Makeig, S., 2004. EEGLAB: an open source toolbox for analysis of single-trial EEG dynamics including independent component analysis. J. Neurosci. Methods 134, 9–21.

Dubreuil-Vall, L., Chau, P., Ruffini, G., Widge, A.S., Camprodon, J.A, 2019. tDCS to the left DLPFC modulates cognitive and physiological correlates of executive function in a state-dependent manner. Brain Stimul 12, 1456–1463.

Frewen, P., et al., 2020. Neuroimaging the consciousness of self: review, and conceptual-methodological framework. Neurosci. Biobehav. Rev. 112, 164–212.

G.lasser, M.F., et al., 2016. A multi-modal parcellation of human cerebral cortex. Nature 536, 171–178.

Golesorkhi, M., et al., 2021a. The brain and its time: intrinsic neural timescales are key for input processing. Commun. Biol. 4, 970.

Golesorkhi, M., Gomez-Pilar, J., Tumati, S., Fraser, M., Northoff, G., 2021b. Temporal hierarchy of intrinsic neural timescales converges with spatial core-periphery organization. Commun. Biol. 4, 277.

Hasson, U., Chen, J., H.oney, C.J., 2015. Hierarchical process memory: memory as an integral component of information processing. Trends Cogn. Sci. 19, 304–313.

H.imberger, K.D., Chien, H.-.Y., H.oney, C.J., 2018. Principles of temporal processing across the cortical hierarchy. Neuroscience 389, 161–174.

H.oney, C.J., et al., 2012. Slow cortical dynamics and the accumulation of information over long timescales. Neuron 76, 423–434.

Huang, Z., Obara, N., Davis, H.(Hap), Pokorny, J., Northoff, G., 2016. The temporal structure of resting-state brain activity in the medial prefrontal cortex predicts self-consciousness. Neuropsychologia 82, 161–170.

Huk, A., Bonnen, K., H.e, B.J., 2018. Beyond trial-based paradigms: continuous behavior, ongoing neural activity, and natural stimuli. J. Neurosci. 38, 7551–7558.

Iemi, L., B.usch, N.A., 2018. Moment-to-moment fluctuations in neuronal excitability bias subjective perception rather than strategic decision-making. eNeuro 5 ENEURO.0430-17.2018.

Iemi, L., Chaumon, M., C.rouzet, S.M., B.usch, N.A., 2017. Spontaneous neural oscillations bias perception by modulating baseline excitability. J. Neurosci. 37, 807–819.

Ito, T., H.earne, L.J., C.ole, M.W., 2020. A cortical hierarchy of localized and distributed processes revealed via dissociation of task activations, connectivity changes, and intrinsic timescales. Neuroimage 221, 117141.

Jiang, M., et al., 2019. Cultural orientation of self-bias in perceptual matching. Front. Psychol. 10, 1469.

Kanwisher, N., Yovel, G., 2006. The fusiform face area: a cortical region specialized for the perception of faces. Philos. Trans. R. Soc. B Biol. Sci. 361, 2109–2128.

K.elley, W.M., et al., 2002. Finding the self? An event-related fMRI study. J. Cogn. Neurosci. 14, 785–794.

K.iebel, S.J., Daunizeau, J., F.riston, K.J., 2008. A Hierarchy of Time-Scales and the Brain. PLoS Comput. Biol. 4, e1000209.

K.olvoort, I.R., Wainio-Theberge, S., Wolff, A., Northoff, G., 2020. Temporal integration as "common currency" of brain and self - scale-free activity in resting-state EEG correlates with temporal delay effects on self-relatedness. Hum. Brain Mapp. 41, 4355–4374.

K.rain, A.L., W.ilson, A.M., Arbuckle, R., C.astellanos, F.X., M.ilham, M.P., 2006. Distinct neural mechanisms of risk and ambiguity: a meta-analysis of decision-making. Neuroimage 32, 477–484.

Limbach, K., C.orballis, P.M., 2016. Prestimulus alpha power influences response criterion in a detection task: prestimulus alpha power influences response. Psychophysiology 53, 1154–1164.

M.acmillan, N.A., C.reelman, C.D., 2005. Detection Theory: a User's Guide, 2nd Ed. May 22, 2022.

M.arkov, N.T., et al., 2014. Anatomy of hierarchy: feedforward and feedback pathways in macaque visual cortex. J. Comp. Neurol. 522, 225–259.

M.urray, J.D., et al., 2014. A hierarchy of intrinsic timescales across primate cortex. Nat. Neurosci. 17, 1661–1663.

M.urray, R.J., Schaer, M., Debbané, M., 2012. Degrees of separation: a quantitative neuroimaging meta-analysis investigating self-specificity and shared neural activation between self- and other-reflection. Neurosci. Biobehav. Rev. 36, 1043–1059.

Nakao, T., et al., 2013. The degree of early life stress predicts decreased medial prefrontal activations and the shift from internally to externally guided decision making: an exploratory NIRS study during resting state and self-oriented task. Front. Hum. Neurosci. 7.

Nakao, T., et al., 2019. From neuronal to psychological noise – Long-range temporal correlations in EEG intrinsic activity reduce noise in internally-guided decision making. Neuroimage 201, 116015.

N.ijhof, A.D., S.hapiro, K.L., Catmur, C., Bird, G., 2020. No evidence for a common self-bias across cognitive domains. Cognition 197, 104186.

Northoff, G., et al., 2006. Self-referential processing in our brain—A meta-analysis of imaging studies on the self. Neuroimage 31, 440–457.

Northoff, G., 2011. Self and brain: what is self-related processing? Trends Cogn. Sci. 15, 186–187.

Northoff, G., 2016. Is the self a higher-order or fundamental function of the brain? The "basis model of self-specificity" and its encoding by the brain's spontaneous activity. Cogn. Neurosci. 7, 203–222.

Northoff, G., Bermpohl, F., 2004. Cortical midline structures and the self. Trends Cogn. Sci. 8, 102–107.

Northoff, G., S.andsten, K.E., Nordgaard, J., K.jaer, T.W., Parnas, J., 2021. The self and its prolonged intrinsic neural timescale in schizophrenia. Schizophr. Bull. 47, 170–179.

Oostenveld, R., Fries, P., Maris, E., Schoffelen, J.M., 2011. FieldTrip: open source software for advanced analysis of MEG, EEG, and invasive electrophysiological data. Comput. Intell. Neurosci. 2011, 1–9.

P.ascual-Marqui, R.D., M.ichel, C.M., Lehmann, D., 1994. Low resolution electromagnetic tomography: a new method for localizing electrical activity in the brain. Int. J. Psychophysiol. 18, 49–65.

Qin, P., et al., 2016. Spontaneous activity in default-mode network predicts ascription of self-relatedness to stimuli. Soc. Cogn. Affect. Neurosci. 11, 693–702.

Qin, P., Northoff, G., 2011. How is our self related to midline regions and the default-mode network? Neuroimage 57, 1221–1233.

Qin, P., Wang, M., Northoff, G., 2020. Linking bodily, environmental and mental states in the self—A three-level model based on a meta-analysis. Neurosci. Biobehav. Rev. 115, 77–95.

R.aut, R.V., et al., 2020. Organization of propagated intrinsic brain activity in individual humans. Cereb. Cortex 30, 1716–1734.

R.eckless, G.E., Bolstad, I., N.akstad, P.H., A.ndreassen, O.A., Jensen, J., 2013. Motivation alters response bias and neural activation patterns in a perceptual decision-making task. Neuroscience 238, 135–147.

Samaha, J., Iemi, L., Haegens, S., B.usch, N.A., 2020. Spontaneous brain oscillations and perceptual decision-making. Trends Cogn. Sci. 24, 639–653.

Smith, D., Wolff, A., Wolman, A., Ignaszewski, J., Northoff, G., 2022. Temporal continuity of self: long autocorrelation windows mediate self-specificity. Neuroimage, 119305.

Sparks, S., C.unningham, S.J., Kritikos, A., 2016. Culture modulates implicit ownership-induced self-bias in memory. Cognition 153, 89–98.

Sui, J., He, X., H.umphreys, G.W., 2012. Perceptual effects of social salience: evidence from self-prioritization effects on perceptual matching. J. Exp. Psychol. Hum. Percept. Perform. 38, 1105–1117.

Sui, J., H.umphreys, G.W., 2015. The Integrative Self: how Self-Reference Integrates Perception and Memory. Trends Cogn. Sci. 19, 719–728.

Tottenham, N., et al., 2009. The NimStim set of facial expressions: judgments from untrained research participants. Psychiatry Res. 168, 242–249.

Tsakiris, M., 2008. Looking for myself: current multisensory input alters self-face recognition. PLoS ONE 3, e4040.

Tsuchiya, N., Wilke, M., Frässle, S., Lamme, V.A.F., 2015. No-report paradigms: extracting the true neural correlates of consciousness. Trends Cogn. Sci. 19, 757–770.

van Vugt, B., et al., 2018. The threshold for conscious report: signal loss and response bias in visual and frontal cortex. Science 360, 537–542.

Winkler, I., Haufe, S., Tangermann, M., 2011. Automatic classification of artifactual ICA–components for artifact removal in EEG signals. Behav. Brain Funct. 7, 30.

Wolff, A., et al., 2019. The temporal signature of self: temporal measures of resting-state EEG predict self-consciousness. Hum. Brain Mapp 40, 789–803.

Wolff, A., et al., 2022. Intrinsic neural timescales: temporal integration and segregation. Trends Cogn. Sci. 26, 159–173.

Yeshurun, Y., Nguyen, M., Hasson, U., 2021. The default mode network: where the idiosyncratic self meets the shared social world. Nat. Rev. Neurosci. 22, 181–192.

Zilio, F., et al., 2021. Are intrinsic neural timescales related to sensory processing? Evidence from abnormal behavioral states. Neuroimage 226, 117579.